Towards a general approach for skeletal muscle DTI acquisition and post-processing

M. Froeling[1,2], A. J. Nederveen[2], M. R. Drost[3], K. Nicolay[1], and G. J. Strijkers[1]

[1]Biomedical NMR, Department of Biomedical Engineering, Eindhoven University of Technology, Eindhoven, Netherlands, [2]Department of Radiology, Academic Medical Center, Amsterdam, Netherlands, [3]Department of Human Movement Science, School for Nutrition, Toxicology and Metabolism, Maastricht University, Maastricht, Netherlands

Introduction: Diffusion tensor imaging (DTI) and fiber tractography of skeletal muscle is challenging for a number of reasons. First short T2 relaxation times result in low SNR and thus limit the resolution. Also the EPI readout leads to susceptibility induced deformation in the images. Furthermore eddy currents and macroscopic motion can lead to a shift of the diffusion weighted volumes with respect to the non-weighted volume. In this study we present a generalized strategy for acquiring and post processing of in vivo skeletal muscle DTI data in order to correct and minimize the above complications. The approach is demonstrated with fiber tractography of skeletal muscle in five regions of the human body at 3T.

DTI: For each body part three acquisitions were performed: dual-echo gradient echo (GE) imaging to derive a B0-field inhomogeneity map, diffusion tensor imaging (DTI) and T1w imaging for anatomy. The FOV (160 to 240 mm square) for all three scans was kept constant as well as the slice thickness (3 to 6 mm, 20 to 65 slices). The image resolution of the GE and DTI measurements varied between 2 and 3 mm whereas the T1w images were acquired with a 1 mm resolution. The acquisition and reconstruction matrix were constant within every acquisition. The voxel volume varied between 20 and 30 mm^3. Further imaging parameters were; T1: TR/TE=512/12ms, NSA=2, voxel size: 1x1 mm^2; GE: $TR/TE_1/TE_2$=12/4.6/9.6ms, NSA=2; DTI: SE-EPI, 15 or 32 evenly spaced gradient directions, TR/TE=8800/(38 to 44)ms, NSA=2, b=400s/mm^2.

Analysis: Post-processing of the data was done with a custom build toolbox for Mathematica 7.0. The workflow of the post-processing is shown in figure 1. Fiber tractography was performed using in house developed software. Tracts start at a seeding ROI and continue bidirectionally with an integration step of 0.1 voxel. Tracts stop when the angle change is greater than 10 degrees per integration step or the FA is less than 0.05 or greater than 0.55. Quantification was done by evaluating the diffusion indices of all voxels which contain fiber tracts.

Results: We compared the 5 sets before and after the proposed post-processing. Figure 2 shows the effect on fiber tractography for the five different regions of the body: lower back, pelvic floor, upper leg, forearm and masticator muscles. Table 1 shows the DTI scalar indices of the tracked volumes depicted in figure 2. Despite an average increase of 30% of the fiber volumes *all* standard deviations and most mean values drop as a result of the processing. However, the changes are relatively small, i.e. 0.05 on average. Changes could be explained by the noise suppression [4-5] and the re-sampling of the data during the post-processing.

Conclusion: We have shown that DTI of skeletal muscle is feasible in various regions of the human body and that the proposed post-processing enhances the quality of the fiber tractography and in general decreases the mean values and standard deviations of the DTI parameters.

Table 1: DTI parameters for the five traced volumes before (white rows) and after (gray rows) post-processing. All values decreased after post-processing except for those in bold.

	Iliocostalis lumborum pars lumborum	pelvic floor	Semi membranosus and tendinosus	Flexor digitorum profundus	Temporalis
λ_1 [10^{-3} mm^2/s]	1.99 ± 0.47	1.86 ± 0.47	2.09 ± 0.52	1.84 ± 0.45	2.22 ± 0.77
	1.77 ± 0.44	1.85 ± 0.42	2.02 ± 0.31	1.79 ± 0.44	2.19 ± 0.71
λ_2 [10^{-3} mm^2/s]	1.43 ± 0.41	1.35 ± 0.37	1.58 ± 0.34	1.44 ± 0.35	1.74 ± 0.68
	1.30 ± 0.36	1.34 ± 0.34	1.57 ± 0.26	1.40 ± 0.36	1.69 ± 0.59
λ_3 [10^{-3} mm^2/s]	1.02 ± 0.36	1.04 ± 0.34	1.23 ± 0.29	1.21 ± 0.32	1.46 ± 0.61
	1.04 ± 0.35	***1.13*** ± 0.32	***1.32*** ± 0.24	***1.21*** ± 0.30	1.39 ± 0.53
MD [10^{-3} mm^2/s]	1.48 ± 0.38	1.42 ± 0.38	1.64 ± 0.34	1.50 ± 0.37	1.81 ± 0.67
	1.45 ± 0.35	***1.64*** ± 0.25	1.47 ± 0.34	1.76 ± 0.59	
FA [-]	0.33 ± 0.12	0.29 ± 0.10	0.26 ± 0.09	0.21 ± 0.08	0.23 ± 0.11
	0.27 ± 0.10	0.25 ± 0.09	0.22 ± 0.07	0.20 ± 0.07	***0.23*** ± 0.10

References: [1] Froeling et al. Proc ISMRM 18 2010: 3240, [2] Haber et al. MICCAI 2007: 9(2): 726-30, [3] Leemans et al. MRM 2009: 61(6): 1336-49, [4] Damon et al. MRM 2008; 60(4): 934-944, [5] Froeling et al. MRM 2010;64(4): 1182-90.

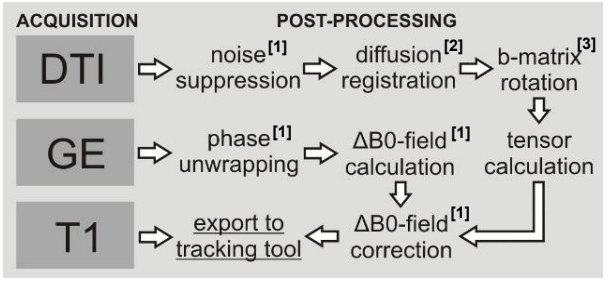

^ **Fig 1:** Data acquisition and post-processing flow chart.

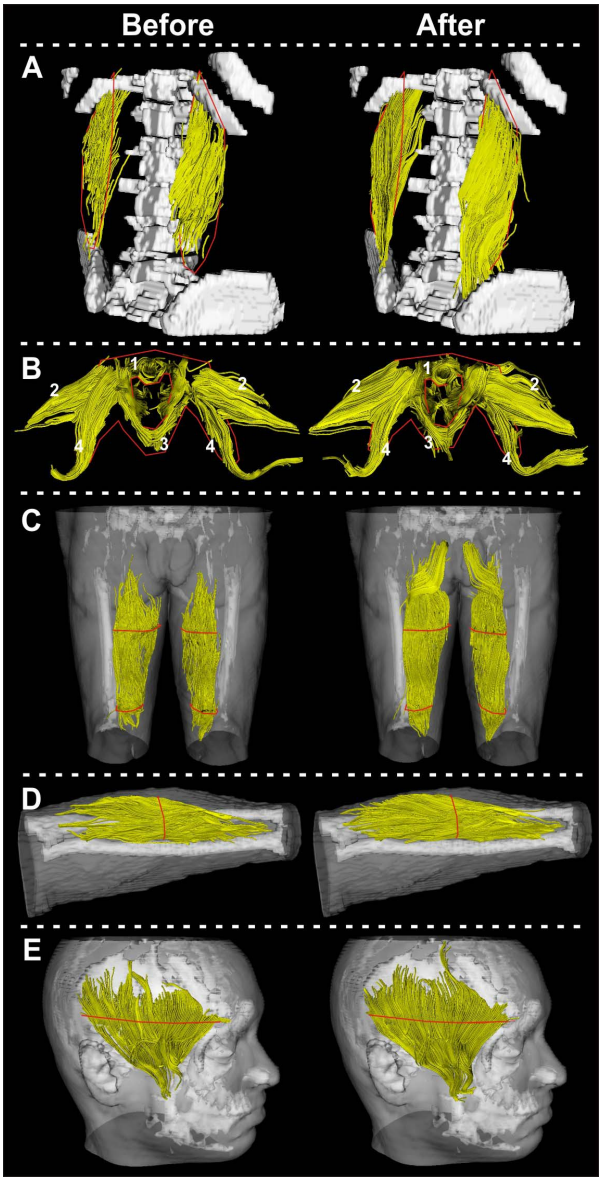

^ **Fig 2:** Fiber tractography in different regions of the human body before and after post-processing. Seeding ROIs are in red. **A)** Iliocostalis lumborum pars lumborum left and right. **B)** Female pelvic floor **1.** urethral sphincter complex **2.** external obturator **3.** pubovisceral components and puborectal sling **4.** internal obturator. **C)** Semimembranosus and tendinosus left and right. **D)** Flexor digitorum profundus. **E)** Temporalis